sistent with hydrodynamical models that predict density fluctuations due to gravitational instabilities on all scales, from the high-density peaks that form galaxies to the distribution of gas in low-density voids (*9–16, 19, 20*). Observation of He II Lyα absorption is the best method to study these regions, and future observations of additional bright quasars with FUSE should provide essential information on the cosmic variance in the structures we see along different lines of sight.

References and Notes

1. J. Gunn, B. Peterson, *Astrophys. J.* **142**, 1633 (1965).
2. R. Lynds, *Astrophys. J.* **164**, L73 (1971).
3. P. Jakobsen *et al.*, *Astrophys. J.* **417**, 528 (1993).
4. P. Jakobsen *et al.*, *Nature* **370**, 35 (1994).
5. A. Songaila, E. M. Hu, L. L. Cowie, *Nature* **375**, 124 (1995).
6. A. F. Davidsen, G. A. Kriss, W. Zheng, *Nature* **380**, 47 (1996).
7. W. Zheng, A. F. Davidsen, G. A. Kriss, *Astron. J.* **115**, 391 (1998).
8. S. R. Heap *et al.*, *Astrophys. J.* **534**, 69 (2000).
9. R. Cen, J. Miralda-Escudé, J. P. Ostriker, M. Rauch, *Astrophys. J.* **437**, L9 (1994).
10. Y. Zhang, P. Anninos, M. L. Norman, *Astrophys. J.* **453**, L57 (1995).
11. ———, A. Meiksin, *Astrophys. J.* **485**, 496 (1997).
12. L. Hernquist, N. Katz, D. H. Weinberg, J. Miralda-Escudé, *Astrophys. J.* **457**, L51 (1996).
13. J. Miralda-Escudé, R. Cen, J. P. Ostriker, M. Rauch, *Astrophys. J.* **471**, 582 (1996).
14. R. A. C. Croft, D. H. Weinberg, N. Katz, L. Hernquist, *Astrophys. J.* **488**, 532 (1997).
15. R. Cen, J. P. Ostriker, *Astrophys. J.* **514**, 1 (1999).
16. R. Davé, L. Hernquist, N. Katz, D. H. Weinberg, *Astrophys. J.* **511**, 521 (1999).
17. H. Bi, *Astrophys. J.* **405**, 479 (1993).
18. ———, J. Ge, L.-Z. Fang, *Astrophys. J.* **452**, 90 (1995).
19. H. Bi, A. F. Davidsen, *Astrophys. J.* **479**, 523 (1997).
20. L. Hui, N. Y. Gnedin, Y. Zhang, *Astrophys. J.* **486**, 599 (1997).
21. M. A. Fardal, M. L. Giroux, J. M. Shull, *Astron. J.* **115**, 2206 (1998).
22. D. Reimers *et al.*, *Astron. Astrophys.* **327**, 890 (1997).
23. A. Smette *et al.*, *Astrophys. J.*, in press (available at http://xxx.lanl.gov/abs/astro-ph/0012193).
24. FUSE covers the wavelength range 912 to 1187 Å with four separate optical channels (*38, 39*). Each channel consists of an off-axis paraboloidal mirror feeding a prime-focus Rowland circle spectrograph. The dispersed light is focused on two 2D photon-counting microchannel-plate detectors with KBr photocathodes that record the time, position, and pulse height of each photon event. Each detector is split into two segments with a small gap between them. Two channels use LiF-coated optics to cover the band 1000 to 1187 Å; the other two channels use SiC coatings to provide short-wavelength coverage down to 912 Å.
25. Because the count rate in a 50,000-s observation in June 2000 was lower than the typical background rate, we chose the dates of these observations to maximize the exposure time during orbital night, the part of the orbit when FUSE is in Earth's shadow. This minimizes the background contribution due to scattered geocoronal Lyα.
26. To obtain the lowest background rate possible, we used only orbital night observations, filtered the high-background "bursts" (*39*) from the data, and used only events with pulse heights in the range 4 to 16. This reduces noise due to the low-pulse-height events that arise from internal detector background rather than from real photons.
27. J. Cardelli, G. Clayton, J. Mathis, *Astrophys. J.* **345**, 245 (1989).
28. D. J. Schlegel, D. P. Finkbeiner, M. Davis, *Astrophys. J.* **500**, 525 (1998).
29. Although the mean opacity is tightly constrained, we note that there is a large dispersion of 0.9 about this value.
30. G. A. Kriss, in *Astronomical Data Analysis Software and Systems III*, D. R. Crabtree, R. J. Hanisch, J. Barnes, Eds., *ASP Conf. Series 61* (Astronomical Society of the Pacific, San Francisco, 1994), p. 437.
31. For the low extinction along this sight line, the interstellar absorption model contributes strong features only for Si II λ1020, Lyβ λ1025, C II λ1036, O I λ1039, Ar I λλ1048, 1066, and no H_2 absorption. Along similar high-latitude sight lines observed with FUSE, the column density in H_2 is on the order of a few $\times 10^{15}$ cm^{-2} [J. M. Shull *et al.*, *Astrophys. J.* **538**, L73 (2000)]. The average opacity produced by such a column density amounts to <4% from 1000 to 1110 Å.
32. A. Songaila, *Astron. J.* **115**, 2184 (1998).
33. W. H. Press, G. B. Rybicki, *Astrophys. J.* **418**, 585 (1993).
34. E. M. Hu, T.-S. Kim, L. L. Cowie, A. Songaila, M. Rauch, *Astron. J.* **110**, 1526 (1995).
35. E. D. Feigelson, P. I. Nelson, *Astrophys. J.* **293**, 192 (1985).
36. P. Madau, F. Haardt, M. J. Rees, *Astrophys. J.* **514**, 648 (1999).
37. W. Zheng, G. A. Kriss, R. C. Telfer, J. P. Grimes, A. F. Davidsen, *Astrophys. J.* **475**, 469 (1997).
38. H. W. Moos *et al.*, *Astrophys. J.* **538**, L1 (2000).
39. D. Sahnow *et al.*, *Astrophys. J.* **538**, L7 (2000).

40. We sadly report that Arthur F. Davidsen, one of our key team members and a pioneer in ultraviolet observations of the IGM, passed away on 19 July 2001. This work is based on data obtained for the Guaranteed Time Team by the NASA-CNES-CSA FUSE mission operated by Johns Hopkins University. Financial support to U.S. participants has been provided by NASA contract NAS5-32985 and by NASA LTSA grant NAG5-7262 to the University of Colorado. A portion of this work is based on observations with the NASA/ESA Hubble Space Telescope, obtained at the Space Telescope Science Institute, which is operated by the Association of Universities for Research in Astronomy Inc. under NASA contract NAS5-26555. These observations are associated with proposal ID 8875. We thank B. Roberts for his efforts in planning and scheduling the successful FUSE observations, and J. Kim for her help in analyzing the STIS data.

21 May 2001; accepted 3 July 2001

No Supermassive Black Hole in M33?

David Merritt,* Laura Ferrarese, Charles L. Joseph

We observed the nucleus of M33, the third-brightest galaxy in the Local Group, with the Space Telescope Imaging Spectrograph at a resolution at least a factor of 10 higher than previously obtained. Rather than the steep rise expected within the radius of gravitational influence of a supermassive black hole, the random stellar velocities showed a decrease within a parsec of the center of the galaxy. The implied upper limit on the mass of the central black hole is only 3000 solar masses, about three orders of magnitude lower than the dynamically inferred mass of any other supermassive black hole. Detecting black holes of only a few thousand solar masses is observationally challenging, but it is critical to establish how supermassive black holes relate to their host galaxies, and which mechanisms influence the formation and evolution of both.

At a distance of 850 kiloparsecs (kpc) from Earth, M33 is classified (*1*) as a late-type ScII-III spiral, consistent with its almost nonexistent bulge (*2, 3*). The nucleus of M33 is very compact, reaching a stellar central mass density of several million solar masses per cubic parsec (*4, 5*), larger than that of any globular cluster. Although such high nuclear densities might be expected in the presence of a supermassive black hole (SMBH) (*6*), ground-based data show no evidence for a central rise in stellar velocities that would indicate the presence of a compact massive object in the nucleus (*4*).

M33 was observed on 12 February 1999 with the Space Telescope Imaging Spectrograph (STIS) on the Hubble Space Telescope (HST). Three sets of two long-slit spectra each, for a total exposure time of 7380 s, were obtained using the G750M grating centered on the CaII absorption triplet near 8561 Å (1 Å corresponds to 10^{-10} m), covering 19.6 km s^{-1} pixel^{-1}. The pixel scale is 0″.05 with a spatial resolution of 0″.115 at 8561 Å. While the two spectra in each set were obtained at the same position to facilitate removal of cosmic ray events, the nucleus was moved along the slit by 0″.216 between each consecutive set. This dithering procedure allows for optimal correction of residual variations in the detector sensitivity as well as identification and removal of malfunctioning pixels. The calibration steps followed the standard procedure (*7*) adopted for STIS observations of the nucleus of M32.

The observed spectrum (Fig. 1) at every resolution element is the convolution of the spectra of individual stars with the line-of-sight velocity distribution (LOSVD) of the stellar ensemble; the latter contains information about the mean and random velocities of stars in the nucleus, projected along the line of sight through the galaxy. We adopted as a typical stellar spectrum that of the K0 III

Department of Physics and Astronomy, Rutgers University, New Brunswick, NJ 08854, USA.

*To whom correspondence should be addressed. E-mail: merritt@physics.rutgers.edu

giant star HD7615, which was observed with the same instrumental configuration. LOSVDs were extracted from the STIS spectra using the Maximum Penalized Likelihood algorithm (*8*) and represented in terms of Gauss-Hermite series (*9*) at every slit position. The mean velocity V_0 and velocity dispersion σ_0 are given [modulo a standard correction applied to V_0 (*9*)] by the first two terms in the Gauss-Hermite expansion. The variation of V_0 and σ_0 with position are shown in Fig. 2.

Neither V_0 nor σ_0 show the rise that would be expected to occur whenever a black hole of mass $M_\bullet$ significantly influences the motion of the stars, i.e., within a distance from the center of the galaxy

$$r_h \equiv \frac{GM_\bullet}{\sigma^2} \approx 0''.028\left(\frac{M_\bullet}{10^4 M_\odot}\right)\left(\frac{\sigma}{20\ \mathrm{km\ s^{-1}}}\right)^{-2} \qquad (1)$$

as seen at the distance of M33. In particular, the central velocity dispersion is 24 ± 3 km s^{-1}, significantly lower than the dispersion of ~35 ± 5 km s^{-1} at ±0″.3 ≈ 1.2 pc. Given the ~0″.05 resolution of STIS, Eq. 1 implies $M_\bullet \lesssim 10^4$ solar masses ($M_\odot$).

The predicted velocities, however, depend not only on $M_\bullet$, but also on the gravitational potential due to the stars and on the form of the stellar orbits around the putative black hole (for example, whether the stellar orbits are eccentric or circular). Therefore, a more rigorous upper limit to the mass of a possible black hole can be derived by constructing realistic dynamical models of the M33 nucleus, which we assume to be spherical on the basis of its projected nearly circular shape (*5*). Although a face-on disk would also project circular isophotes, the position angle and ellipticity of the nucleus and the outer disk are considerably different, implying that the former is unlikely to be a simple extension of the latter. Furthermore, the properties of the M33 nucleus are consistent with those observed for globular clusters (*4*)—the prototypical spherical systems. The luminosity density was represented by (*2, 5, 10*)

$$\nu(r) = \nu_0\left(\frac{r}{a}\right)^{-\gamma}\left(1 + \frac{r}{a}\right)^{\gamma-4} \qquad (2)$$

In the above equation, a is the distance from the center of the galaxy at which the luminosity density is a fraction (in our case, one-quarter) of the central value ν_0, whereas γ defines the gradient in the luminosity density for $r \ll a$. We adopt $\gamma = 2$ and $a = 1$ kpc (*5*); ν_0 was fixed by requiring the luminosity within 1 pc of the center to be $1.0 \times 10^6\ L_\odot$. The gravitational potential due to the stars was derived from $\nu(r)$ and from Poisson's equation as a function of the parameter M/L, the ratio of stellar mass to V-band luminosity expressed in solar units. Past studies found $M/L \lesssim 0.5$ suggestive of a young stellar population (*4, 11*).

For a dynamically relaxed stellar system in a spherical gravitational potential, the number of stars that occupy a given location in velocity-position space may be any non-negative function $f(E,l)$ of the orbital energy E and angular momentum l. We used standard techniques (*12*) to find the f which best reproduced the kinematical data given $M_\bullet$ and M/L, subject to the constraint that the integral of f over velocities reproduced the assumed luminosity density $\nu(r)$. The velocities predicted by f were projected onto the plane of the sky and convolved with the HST point spread function (PSF) and the STIS slit in order to allow direct comparison with the observed velocities. We emphasize that a two-integral [$f(E,L)$] model for a spherical system, like the model adopted here, permits precisely as much flexibility in the orbital distribution as a three-integral model for an axisymmetric system. In other words, the constraints on the mass of the M33 SMBH derived from a three-integral modeling code would be precisely the same as those found here, unless the underlying stellar potential were assumed to be significantly nonspherical.

In the absence of any additional constraints on f, we found that even black holes with $M_\bullet \gtrsim$ 50,000 $M_\odot$ could be made consistent with the data. However, the f's corresponding to these large values of $M_\bullet$ were always found to be physically unreasonable: the stellar orbits changed suddenly from nearly circular at $r \gtrsim$ 0.1 pc to nearly radial at $r \lesssim 0.1$ pc, causing the projected velocity dispersion to drop sharply at a radius corresponding to the angular size of the STIS PSF before rising again near the black hole. After convolution with the PSF, the observed velocities in these solutions therefore

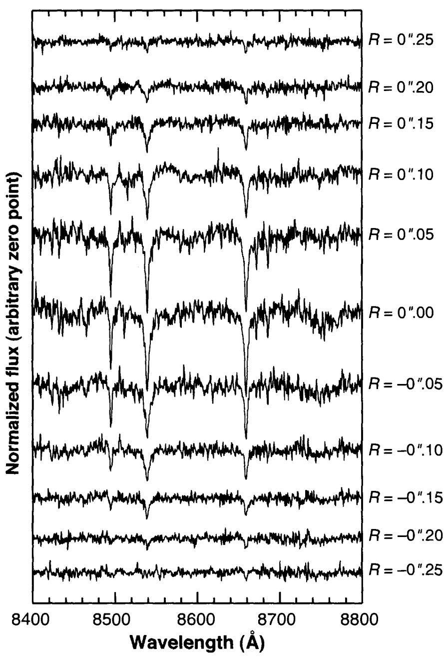

Fig. 1. HST/STIS spectra of M33 extracted at the location of the nucleus of the galaxy (central row, marked R = 0″.00) and up to 0″.25 (1.0 pc) off-nucleus. The spectra have been shifted by an arbitrary amount in the vertical direction, but the same scale has been maintained. The decrease in the velocity dispersion of the CaII absorption lines (~8550 Å) at the central positions is visible.

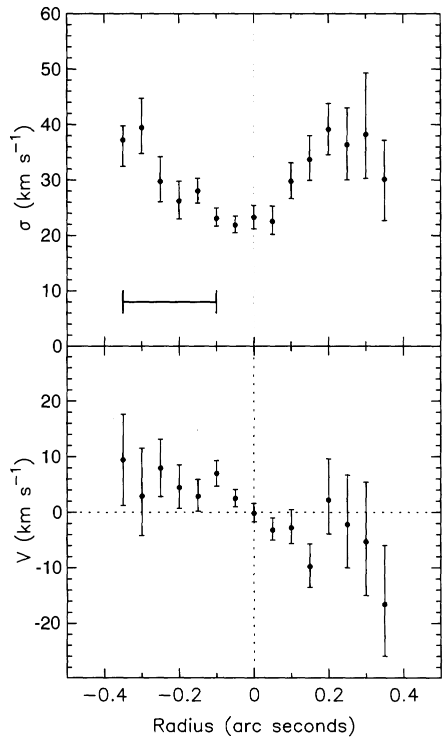

Fig. 2. The stellar rotation curve (lower panel) and velocity dispersion profile (upper panel) of stars in the nucleus of M33, derived from the STIS spectra as described in the text. Error bars (1σ) are shown. Also shown is the angular scale corresponding to 1 pc at the distance of M33.

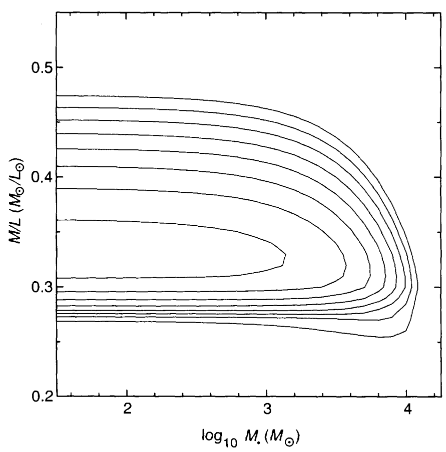

Fig. 3. Contours of constant $\tilde{\chi}^2$ measuring the fit of the dynamical models described in the text to the data of Fig. 2. Horizontal axis is the assumed mass of a central black hole and vertical axis is the mass-to-light ratio of the stars in the bulge. The lowest plotted contour is at $\chi^2 = 1.4$, and contours are separated by 0.2.

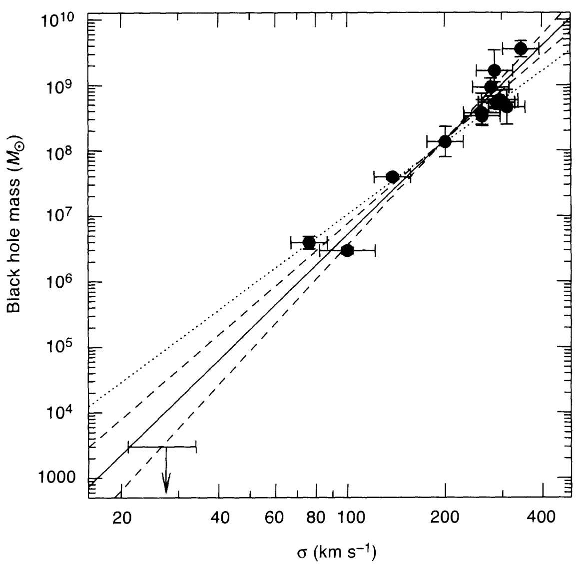

Fig. 4. The thick solid line represents the $M_\bullet-\sigma$ relation as derived by Ferrarese and Merritt (*14*), with 1$-\sigma$ confidence limits on the slope shown by the dashed lines. The upper limit for the black hole mass in M33 (shown by the arrow) is consistent with this relation, but is inconsistent with the shallower relation advocated by Gebhardt *et al.* (*15*), shown by the thin dotted line.

remained low even when $M_\bullet$ was large. To avoid such unphysical behavior, the solutions for f were regularized (*12*), i.e., forced to be smooth: The regularization parameter was chosen to be just large enough to suppress unphysical features on the scale of the PSF.

Even after regularization, reasonable fits to the data with $M_\bullet \gtrsim 10{,}000\ M_\odot$ could still be found for values of the stellar-mass-to-light ratio lower than 0.1 $M_\odot/L_\odot$. This can be understood qualitatively as follows: The gravitational potential is defined by the joint contribution of the stars and the central black hole. Decreasing the stellar-mass-to-light ratio has the effect of diminishing the stellar contribution to the central potential; to compensate, the mass of the black hole needs to be increased proportionally. Decreasing M/L also has the more subtle effect of requiring the stellar orbits to become predominantly radial at large distances. As a result, the predicted line-of-sight velocity dispersion drops suddenly just outside of the fitted region, contrary to what is observed: the velocity dispersion in the M33 bulge appears to remain high, $\sigma \approx 34$ km s^{-1}, within $R \approx 80''$ (*13*). By forcing the rms line-of-sight velocity to be greater than 30 km s^{-1} in the radial range $0''.5 < R < 20''$, such unphysical solutions are excluded.

The best-fit f subject to these constraints was computed over a grid of ($M_\bullet$,M/L) values (Fig. 3). For $M_\bullet \lesssim 1000\ M_\odot$ and $M/L \approx 0.35$, the mass of the putative black hole is too small to significantly affect the observable velocities, and the quality of the fit is independent of $M_\bullet$. As $M_\bullet$ is increased above ~2000 $M_\odot$, $\tilde{\chi}^2$ increases as the rise in the central value of σ provides a progressively worse fit to the data at $R \lesssim 0''.1$. Values of $M_\bullet$ as large as ~3000 $M_\odot$ imply $\tilde{\chi}^2 \approx 1.7$ when only the data in the innermost two or three points are compared with the model, and produce a best-fit model that overpredicts the velocity dispersion at each of the four innermost points by about twice the measurement uncertainty in σ. We take 3000 $M_\odot$ as our upper limit on $M_\bullet$. This value is roughly 10 times smaller than the value of ~$5 \times 10^4\ M_\odot$ inferred from ground-based data (*4*).

There is an empirical relation between the masses of SMBHs and the properties of their host bulges, called the "$M_\bullet$–σ relation," which is expressed as (*14*)

$$\frac{M_\bullet}{10^8\ M_\odot} \approx 1.3 \left(\frac{\sigma_c}{200\ \mathrm{km\ s^{-1}}}\right)^\alpha \qquad (3)$$

with $\alpha = 4.80 \pm 0.54$. Here, σ_c is the stellar velocity dispersion measured within an aperture of radius $r_e/8$ centered on the nucleus and r_e is the projected radius containing 1/2 of the light of the bulge. Because r_e is not well measured for the M33 bulge [estimates range from 0.5 kpc (*2*) to 2 kpc (*10*)] and the dependence of σ on radius is not known accurately outside of the central ~1 pc, we conservatively adopt 21 km s^{-1} $\leq \sigma_c \leq$ 34 km s^{-1}, the range of values measured between 0″s and 80″s (*13*). The $M_\bullet$–σ relation then predicts a mass in the range $2600 \leq M_\bullet/\mathrm{M}_\odot \leq 26{,}300$, consistent with our upper limit. In contrast, the shallower $M_\bullet$–σ relation proposed by Gebhardt *et al.* (*15*) would imply $M_\bullet \gtrsim 2.5 \times 10^4\ M_\odot$, which is not consistent with the upper limit on $M_\bullet$ obtained here.

The $M_\bullet-\sigma$ relation is used to study SMBH demographics and constrain models of black hole formation and evolution (*16–18*). The low-mass end of the relation is of particular importance because SMBHs larger than ~10^6 $M_\odot$ are believed to originate through physical processes different from those regulating the formation of smaller mass black holes (*19, 20*). However, all SMBHs detected so far have masses $M_\bullet > 10^6\ M_\odot$ (Fig. 4). Evidence for "intermediate-mass black holes" (IMBHs), with masses in the range of $10^2\ M_\odot \lesssim M_\bullet \lesssim 10^5\ M_\odot$, is so far only circumstantial and relies on speculations concerning the nature of the super-luminous off-nuclear x-ray sources (ULXs) detected in a number of starburst galaxies (*21, 22*). The connections between the possible black hole in M33 and ULXs is tantalizing: the M33 nucleus itself contains the brightest ULX in the Local Group (*23*) and has optical and near-infrared colors and spectra consistent with those of a young cluster (*3*), with size and mass similar to those measured for the cluster containing the brightest of the M82 ULXs (*5, 24*). However, because our upper limit on $M_\bullet$ in M33 is consistent with the $M_\bullet-\sigma$ relation as defined by much brighter galaxies, we cannot yet conclude that the presence of a black hole in M33 would require a different formation mechanism from that of the SMBHs detected in other galaxies.

Note added in proof: While this paper was in press, an independent study of the kinematics of the M33 nucleus (*25*) was submitted. A critical comparison of the results of the two studies will be presented in a forthcoming paper (*26*).

References and Notes

1. S. van den Bergh, *Ann. Rev. Astron. Astrophys.* **9**, 273 (1999).
2. D. Minniti, E. W. Olszewski, M. Rieke, *Astrophys. J.* **410**, L79 (1993).
3. S. van den Bergh, *Publ. Astron. Soc. Pac.* **103**, 609 (1991).
4. J. Kormendy, R. D. McClure, *Astron. J.* **105**, 1793 (1993).
5. T. R. Lauer, S. M. Faber, E. A. Ajhar, C. J. Grillmair, P. A. Scowen, *Astron. J.* **116**, 2263 (1998).
6. R. van der Marel, *Astron. J.* **117**, 744 (1999).
7. C. Joseph *et al.*, *Astrophys. J.* **550**, 668 (2001).
8. D. Merritt, *Astron. J.* **114**, 228 (1997).
9. R. P. van der Marel, M. A Franx, *Astrophys. J.* **407**, 525 (1993).
10. M. W. Regan, S. N. Vogel, *Astron. J.* **434**, 536 (1994).
11. T. Takamiya, Y. Sofue, *Astrophys. J.* **534**, 670 (2000).
12. D. Merritt, *Astrophys. J.* **413**, 79 (1993).
13. D. Minniti, *Astron. Astrophys.* **306**, 715 (1996).
14. L. Ferrarese, D. Merritt, *Astrophys. J.* **539**, L9 (2000).
15. K. Gebhardt *et al.*, *Astrophys. J.* **539**, L13 (2000).
16. M. G. Haehnelt, G. Kauffmann, *Mon. Not. R. Astron. Soc.* **318**, L35 (2000).
17. L. Ciotti, T. S. van Albada, *Astrophys. J.* (http://xxx.lanl.gov/abs/astro-ph/0103336), in press.
18. D. Merritt, L. Ferrarese, *Mon. Not. R. Astron. Soc.* **320**, L30 (2001).
19. M. G. Haehnelt, P. Natarajan, M. J. Rees, *Mon. Not. R. Astron. Soc.* **308**, 77 (1998).
20. M. C. Miller, D. P. Hamilton (http://xxx.lanl.gov/abs/astro-ph/0106188), in preparation.
21. H. Matsumoto *et al.*, *Astrophys. J.* **547**, L25 (2001).
22. G. Fabbiano, A. Zezas, S. S. Murray, *Astrophys. J.* (http://xxx.lanl.gov/abs/astro-ph/0102256), in press.
23. K. S. Long, S. Dodorico, P. A. Charles, M. A. Dopita, *Astrophys. J.* **246**, L61 (1981).
24. T. Ebisuzaki *et al.* (http://xxx.lanl.gov/abs/astro-ph/0106252), in preparation.
25. K. Gebhardt *et al.* (http://xxx.lanl.gov/abs/astro-ph/0107135), in preparation.
26. M. Valluri *et al.*, in preparation.

27. Supported by NSF through grant 4-21911, and by NASA through grants 4-21904 and NAG5-8693.

28 June 2001; accepted 11 July 2001
Published online 19 July 2001;
10.1126/science.1063896
Include this information when citing this paper.